

# Development of an Access Charge Framework for High-Speed Rail Incorporating Rail Replacement Costs

Nitesh Kumar Yadav<sup>ID</sup>, Mohamed Kaseko, Hualiang Teng

Department of Civil and Environmental Engineering and Construction, University of Nevada Las Vegas, Las Vegas, USA  
Email: yadavn2@unlv.nevada.edu, mohamed.kaseko@unlv.edu, hualiang.teng@unlv.edu

**How to cite this paper:** Yadav, N.K., Kaseko, M. and Teng, H. (2026) Development of an Access Charge Framework for High-Speed Rail Incorporating Rail Replacement Costs. *Journal of Transportation Technologies*, 16, 166-191.

<https://doi.org/10.4236/jtts.2026.161011>

**Received:** December 15, 2025

**Accepted:** January 16, 2026

**Published:** January 19, 2026

Copyright © 2026 by author(s) and Scientific Research Publishing Inc.  
This work is licensed under the Creative Commons Attribution International License (CC BY 4.0).

<http://creativecommons.org/licenses/by/4.0/>



Open Access

## Abstract

Shared high-speed rail corridors present a growing challenge for cost allocation as multiple operators use the same infrastructure under open-access or cooperative arrangements. Traditional access charge systems often rely on generalized usage metrics, such as train-kilometers or gross tonnage, which do not explicitly account for the effects of train speed and track geometry on infrastructure wear. As a result, these simplified approaches overlook the true contribution of dynamic forces to rail degradation, leading to potential under- or over-recovery of costs among operators. This motivates the need for a technically grounded framework that links measurable train and track parameters to rail replacement costs for equitable cost sharing. The proposed framework builds on the static rail replacement threshold traditionally used by infrastructure managers and extends it to incorporate the effects of train speed, axle load, and track geometry. It first determines the cumulative tonnage threshold for rail replacement by combining static, dynamic, and lateral loads acting on the rail. This threshold is then used as the basis for estimating the service life of the rail under shared operations, where different train types operate over the same segment. The total rail replacement cost is distributed among the operators according to their proportionate contribution to the cumulative loading during the rail's service life, resulting in an equitable, load-based access charge for each service. A case study of the Palmdale-Burbank segment of the California High-Speed Rail corridor, currently under construction and expected to be shared with the privately operated Brightline West, demonstrates the application of the proposed framework. The case study used publicly available and assumed operating data of the two train systems. The analysis shows that the heavier, faster train (CAHSR) contributes a greater share of total rail wear and therefore incurs a higher per-trip access charge than the lighter, slower Brightline West train service. The analysis also revealed that neglecting

the effects of dynamic and lateral loads would overestimate the rail service life by nearly a factor of two, underscoring the importance of accounting for these forces in both maintenance forecasting and cost allocation. These findings confirm that incorporating speed, axle load, and geometry effects provide a more accurate and equitable basis for allocating maintenance and renewal costs in shared high-speed rail operations.

### Keywords

High-Speed Rail, Track Access Charge, Rail Replacement, Dynamic Loads, Cost Allocation, Shared Corridors

---

## 1. Introduction

High-speed rail delivers fast, reliable, high-capacity intercity travel. Systems operate at more than 250 km/h on new lines or around 200 km/h on upgraded lines, enabled by advanced infrastructure, rolling stock, and signaling [1]. The first modern system, Japan's Shinkansen in 1964, showed that high-speed rail can relieve corridor capacity constraints while maintaining an exceptional safety record and very high ridership [2]. Successful adoption followed in France, Germany, Spain, Italy, the United Kingdom, China, and South Korea, driven by goals of shorter travel times, added capacity, and regional development.

As networks expanded, many countries began allowing multiple operators to use the same infrastructure. Shared use aims to utilize costly assets and fair access under transparent rules. However, this arrangement also creates new challenges for pricing track access, to ensure that each user pays in line with the wear they cause.

Track access charges are the fees paid by train operators to run on a network. The guiding principle is cost causation: users should cover the costs directly attributable to their operations. European policy mandates that charges for minimum access package reflect the cost directly caused by each train service, and regulators emphasize transparency and non-discrimination [3]. In particular, the main contributor to rail maintenance costs is the damage caused by the loads of passing trains. Higher axle loads, greater speeds, and dynamic forces increase stress, accelerate wear, and shorten the rail's service life [4].

However, while these principles establish the foundation for fair cost allocation, most current access charge systems rely on broad cost categories that do not explicitly account for how train-induced loads translate into actual rail deterioration. In this study, rail replacement is selected as the initial focus of cost allocation because rail wear is directly governed by cumulative wheel-rail loading and represents a major renewal cost on high-speed rail corridors. Rail life is commonly expressed in terms of cumulative tonnage thresholds, making it well suited for integration with load-based deterioration modeling. Focusing on rail replacement establishes a clear and physically grounded link between train-induced loads, con-

sumption of service life, and renewal cost allocation. Other track components, such as ballast and sleepers, while also critical to track performance, involve additional deterioration mechanisms and maintenance practices and are therefore beyond the scope of the present framework and left for future extension. To ensure that each operator pays in proportion to the wear they cause, it is necessary to quantify rail degradation in measurable terms, particularly rail service life and the associated replacement cost. Linking physical damage mechanisms to economic cost recovery enables a more transparent and usage-based access charge structure.

In current practice, rail life is often measured in terms of cumulative static tonnage. These thresholds are expressed in million gross tonnes (MGT) based on long operating experience. For example, the Shinkansen uses a threshold of approximately 600 MGT, with similar limits reported on other high-speed systems [5]. While practical, such thresholds do not isolate the effects of train speed or dynamic behavior. Research shows that at high speeds, dynamic wheel loads can far exceed static loads, accelerating degradation of the rail head and near-surface layers [6]. When multiple trains with varying axle loads, speeds, frequencies, and wheelset counts share a corridor, a static-tonnage rule alone cannot reveal each train's true contribution to rail wear. This undermines the fairness of cost allocation.

This study addresses that gap. The objective is to develop a framework for allocating rail replacement costs on shared high-speed corridors, accounting for both static and dynamic wheel-rail forces. The framework builds upon and extends earlier work developed by the author in a master's thesis, with refinements to the formulation and presentation for journal dissemination [7]. The framework links axle load, train speed, service frequency, number of wheels, and track curvature to the total load imposed on the rail. These calculated loads are then used to estimate a cumulative tonnage threshold for rail replacement and the corresponding service life of the track segment. It then converts the rail renewal cost into an equivalent annual cost, assigning that cost to each operator in proportion to their calculated usage impact. The outcome is a per-trip access charge for each service that reflects its actual infrastructure usage.

The scope is limited to the rail component of the track structure. Ballast, sleepers, fasteners, and subgrades are not modeled. Static loading is derived directly from axle weight. Dynamic effects are estimated with semi-empirical relations that account for factors like speed, curve radius, track gauge, and superelevation deficiency. The method yields the maximum cumulative traffic (tonnage) the rail can sustain before requiring renewal, then annualizes the replacement cost using life-cycle cost principles and applies a proportional cost-sharing rule. A representative case study with two high-speed train types illustrates how the framework would operate on a planned shared-use corridor.

The contribution is twofold. First, it explicitly incorporates the role of speed and dynamic forces into a tonnage-based policy framework already familiar to practitioners. Second, it provides an access charge calculation aligned with actual physical impact, thereby supporting equity, transparency, and sustainable mainte-

nance funding for high-speed rail corridors.

## 2. Literature Review

### 2.1. Rail Degradation Types in High-Speed Rail

Operation at high-speed subjects the track to large, repeated vertical loads. The principal deterioration mechanisms are rail wear, rolling contact fatigue, track-geometry deterioration driven by ballast and subgrade settlement, and damage from dynamic impacts [8]. Rail wear is the progressive loss of metal at the rail head caused by wheel-rail friction and abrasion. Wear is most severe on curves and under higher axle loads, and it alters the rail profile until grinding or renewal is required. Rolling contact fatigue consists of crack initiation and growth in rail steel under many stress cycles. Typical manifestations include head checks and shelling. Without timely grinding, these cracks can coalesce and lead to fractures. Track-geometry deterioration arises from the deformation and settlement of ballast and subgrade under dynamic loading. Repeated traffic produces voids and differential settlement that must be corrected through tamping and lining to maintain alignment, level, and gauge. Dynamic impact damage occurs when wheel or track defects such as wheel flats, out-of-round wheels, dipped welds, or joints generate short-duration, high-magnitude forces. These impacts accelerate wear and fatigue in both rail and ballast.

These mechanisms are interdependent. As geometry quality declines, the amplitude of dynamic wheel forces increases; the elevated dynamics then accelerate rail wear and fatigue, which further degrades geometry. Evidence from lines designed for speeds up to 350 km/h shows that vertical wheel forces are the primary driver of geometry deterioration at very high speeds. Modern trainsets with lower axle load and improved suspension reduce these forces, and field measurements on a 350 km/h corridor demonstrate that, together with elastic components such as flexible rail pads, these vehicle improvements can hold geometry deterioration at levels comparable to 300 km/h operation [9].

From a maintenance-cost perspective, track settlement and the resulting geometry loss are often the dominant drivers. Studies that separate the contributions of wear, rolling contact fatigue, and settlement find that geometry-related interventions, principally tamping and ballast rehabilitation, consume the largest share of expenditure because they recur frequently and are tied to ride quality and safety [3]. Wear and fatigue remain important but are more readily managed through routine grinding and planned rail replacement.

To relate traffic to deterioration, engineers employ empirical and semi-mechanistic models. Simple formulations link the decline of geometry quality to cumulative tonnage. More detailed approaches distinguish four categories of vertical forces: low-frequency car-body ride forces, higher-frequency wheel-rail interaction forces associated with bogie and suspension dynamics, impact forces due to wheel or track irregularities, and static wheel loads [10]. Each category contributes differently to damage, which is why technical standards limit both axle load and

dynamic augment. Research in the United Kingdom further recommended an explicit limit on maximum dynamic wheel force, to complement static axle-load limits and prevent outlier vehicles from imposing extreme forces [10].

In summary, deterioration of high-speed track is cumulative and governed by the magnitude and frequency of vertical force. Rail wear, rolling contact fatigue, and settlement are closely linked through their shared dependence on dynamics. Although modern vehicles and elastic track components mitigate these effects, regular maintenance remains essential. A cost-allocation framework that reflects measured or predicted loads is therefore consistent with the way infrastructure deteriorates in service.

## **2.2. Track Access Charging Practices and Cost Recovery Frameworks**

Track access charges allocate infrastructure costs to operators in proportion to use. The design of these systems reflects economic efficiency and policy goals such as fair competition and cost recovery [3]. Frameworks differ in structure and scope, but most include a variable component linked to wear-and-tear and, in many cases, mark-ups to cover fixed costs.

### **European model: marginal cost with mark-ups**

EU legislation requires charges for the minimum access package to reflect the incremental cost of running trains [3]. This aligns payments with the damage each service causes and encourages track-friendly vehicles through differentiation by vehicle type. Implementation often relies on proxies such as gross tonne-kilometers, axle-load classes, and speed bands. Mark-ups are permitted to recover fixed costs provided they do not unduly suppress demand. Recovery levels vary by country. One assessment reported that about 91% of the German high-speed charge reflected capital cost mark-ups, with 9% covering direct variable cost [11]. The cost base can include maintenance and renewal, capacity opportunity costs, congestion, and in some systems externalities such as environmental or accident risk. On saturated lines, peak or route-specific surcharges address scarcity of capacity.

### **Swiss “base price wear” approach**

Switzerland’s 2017 train-path pricing introduced a vehicle-specific “base price wear” that converts measured or specified vehicle-track interaction into a per-kilometre cost [12]. The formulation links damage to variables such as dynamic wheel force, traction power, specific track friction energy, and vertical and lateral forces in switches. Damage laws are calibrated to costs and applied across track categories defined by curvature and speed, so the charge varies by train type and by segment characteristics [13]. The aim is cost-reflective pricing and incentives to reduce damaging forces.

### **Other frameworks and the U.S. context**

Outside Europe, vertically integrated systems often treat access charges as internal transfers. Where infrastructure and operations are separate, explicit TACs

are needed. In the United States, historic agreements on freight-owned corridors were negotiated rather than damage-based. Emerging high-speed projects have prompted formal estimation of usage-based charges. A simulation study for a California segment reported an operations-and-maintenance fee of about \$14.61 per train-mile at planned frequencies, excluding capital recovery [11]. A regression study using international data estimated a baseline of \$6.30 per train-mile for the full corridor initial plan [14]. Differences reflect methodology and scope, and both studies show that adding renewal and capital recovery would raise total charges.

### **2.3. Modelling and Simulation Approaches for Load-Based Damage Estimation**

Implementing a load-based access charge requires estimating the damage and cost attributable to each train. Literature groups methods into engineering models and econometric models, with hybrid approaches that combine both to improve accuracy [3].

#### **Engineering simulation models**

These models compute damage from vehicle and track inputs such as axle load, suspension, wheel profile, curve radius, and track structure. Multi-body simulations provide dynamic wheel-rail forces that feed wear, fatigue, or settlement relations [8]. The Swiss track deterioration model developed at Graz University outputs component-level damage values and underpins the Swiss charging approach; its wear formulation is calibrated so the summed damage across trains matches observed maintenance outlays on reference lines. Very detailed physics are impractical for routine charging, while simple proxies like gross tonnage ignore speed and unsprung mass. The Swiss approach uses a small set of measurable variables, including dynamic wheel force, traction power, and specific track friction energy, to produce a per-train, cost-oriented damage metric [15].

#### **Econometric cost models**

These models relate observed maintenance or renewal costs to usage on real networks. A classic analysis linked costs to traffic levels to estimate a cost per gross-ton-kilometre for wear and tear [16]. Such models capture many influences implicitly but are weaker at attributing costs to specific mechanisms or vehicle types on mixed-traffic corridors.

#### **Hybrid engineering-econometric models**

Hybrid methods first create engineering indices for wear, rolling contact fatigue, and settlement based on the vehicle mix and operating conditions, then regress observed costs on those indices [3]. Results show the settlement index has the largest marginal cost impact, followed by rolling contact fatigue, then wear. This enables cost attribution by vehicle type and supports differentiated charging grounded in measured damage contributions.

#### **Current and emerging tools**

Recent programmes provide damage functions that relate geometry degradation to tonnage with modifiers for speed and axle load, and category-based charges

that assign vehicles to damage bands. Trends include wider use of dynamics outputs, traction and braking effects, and short-wave irregularity influences on rolling contact fatigue. Statistical forms such as t-Gamma distributions are explored to better fit deterioration data [8]. The goal is to expand explanatory power while keeping models usable for charging and to incentivize lower impact rolling stock design.

## **2.4. Economic and Regulatory Context of Shared High-Speed Corridors**

Early high-speed railways were typically planned, owned, and operated by a single national entity. European reforms shifted this model toward open access by separating infrastructure management from operations and requiring transparent, non-discriminatory access and pricing [3]. Independent regulators review cost bases and oversee compliance to protect competition and service quality.

Pricing in this setting balances two goals: recovering sufficient revenue for maintenance and renewals while keeping charges low enough to sustain viable services. EU rules permit mark-ups above marginal cost where it is justified and non-discriminatory. The resulting cost recovery system varies by country. Some networks incorporate a substantial capital component in access charges, while others keep charges closer to direct costs and rely more on public funding [11].

Outside Europe, access arrangements are more heterogeneous. In Japan, vertically integrated Shinkansen companies handle infrastructure and operations, with negotiated internal settlements where sharing occurs on conventional lines. In the United States, shared-use agreements exist on intercity and commuter corridors, and structured cost-allocation frameworks such as those on the Northeast Corridor provide an analogue to formal access charging for passenger services [17]. As new high-speed projects mature, more explicit, load-sensitive charging frameworks will be required.

## **3. Methodology**

One of the key inputs in the proposed framework is the cumulative axle load policy for rail replacement. This is the total allowable cumulative load that the rail is subjected to before being replaced. Shimatake [5] surveyed several highspeed rail systems in four different countries and reported their policies in terms of the cumulative tonnage for rail replacement. Depending on the type of rail used, the values ranged from 150 to 600 MGT (Megatons). For a given highspeed rail system, the proposed methodology converts this cumulative static load into equivalent total cumulative static and dynamic load that takes into account the dynamic and curvature-induced effects of the train passage on a rail track.

### **3.1. Calculation of Rail Replacement Cumulative Threshold ( $Q_{\max}$ )**

The rail replacement access charge framework developed in this study applies the method of Guerrieri [18], for calculating the overall wheel-rail loading of a train.

Using this computed load, the maximum cumulative tonnage threshold for rail replacement is subsequently derived. In this approach, wheel-rail load is decomposed into static load due to train's weight distributed through each wheelset, and the dynamic load arising from motion effects amplified by speed, suspension response, and track irregularities. In addition to vertical forces, lateral loads generated during curve negotiation are also incorporated, representing the combined effects of centrifugal forces and wheel-flange contact. The resultant wheel-rail load is then determined by vectorially combining the total vertical and lateral components, providing a more comprehensive representation of the stress state experienced by the rail.

The framework assumes that rail wear accumulation is directly proportional to the calculated resultant wheel-rail load. Under this assumption, higher resultant loads correspond to proportionally higher rates of rail deterioration and faster consumption of the rail's cumulative load capacity. This simplification is consistent with cumulative tonnage-based rail replacement policies currently used by infrastructure managers and provides a practical basis for allocating rail replacement costs according to each train's relative contribution to loading.

Track geometry adds further complexity: although tangent segments experience both static and dynamic forces, curved segments additionally carry curvature-induced and lateral forces generated by centrifugal effects and flange contact. These additional stresses in the curve govern the location for wear of the rail. Because available data seldom indicates whether tangent and curved rail portions are renewed separately, this study assumes that rail replacement is triggered when the curve segments, which are more critical in terms of loading, reach the end-of-life load threshold and all the rail segments, including the tangent segments, are replaced at the same time. All subsequent calculations of cumulative load and service life are therefore based on curved-segment conditions.

**Figure 1** illustrates the key vertical and lateral forces acting on the wheel-rail interface on a curved section of the trail track. It shows how centrifugal and gravitational forces interact with superelevation to produce unequal inner and outer wheel loads. From the figure, the relevant parameters that are used in the analytical proposed framework include:

$P$  = the axle load.

$Q_e$  = the vertical force on the outer rail.

$Y_e$  = the lateral force on the outer rail.

$h$  = track superelevation.

$s$  = track gauge.

$P_c$  = the vertical distance from the rail head plane to the vehicle's center of gravity.

**Figure 2** is the flowchart showing the steps used in determination of the maximum rail load threshold for a high-speed rail line system. The procedure is divided into two sections.

In section A, the service life of the rail is made based on operating static wheel

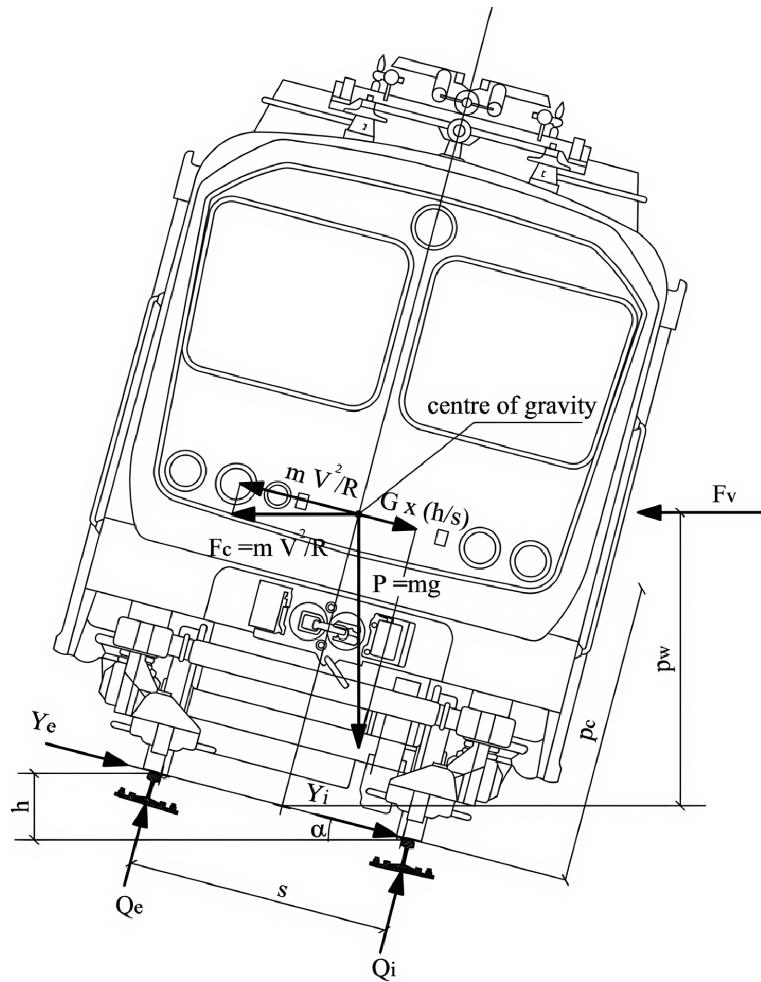


**Figure 1.** Schematic of train on curved track showing parameters used in vertical load calculations (adapted from Guerrieri [18]).

loads, the operating frequency and the policy static-load threshold. Then in section B, analysis is extended by incorporating additional train and track parameters to determine the combined curvature-induced dynamic effects of the vertical and lateral loading on the rail and the result is the cumulative total load threshold for rail replacement,  $Q_{max}$ .

Below are the steps for calculation of the different components leading to the maximum cumulative tonnage threshold:

A. Calculate service life from static load lifetime threshold.

Step 1: Static load per wheel

$$Q_{st} = 0.5P \tag{1}$$

where  $P$  is the axle load. Each axle has two wheels.

Step 2: Service life of the rail

$$N_L = Q_{threshold} / (Q_{st} * n) \tag{2}$$

where  $Q_{threshold}$  = rail replacement threshold tonnage.

$Q_{st}$  = static load per wheel per rail.

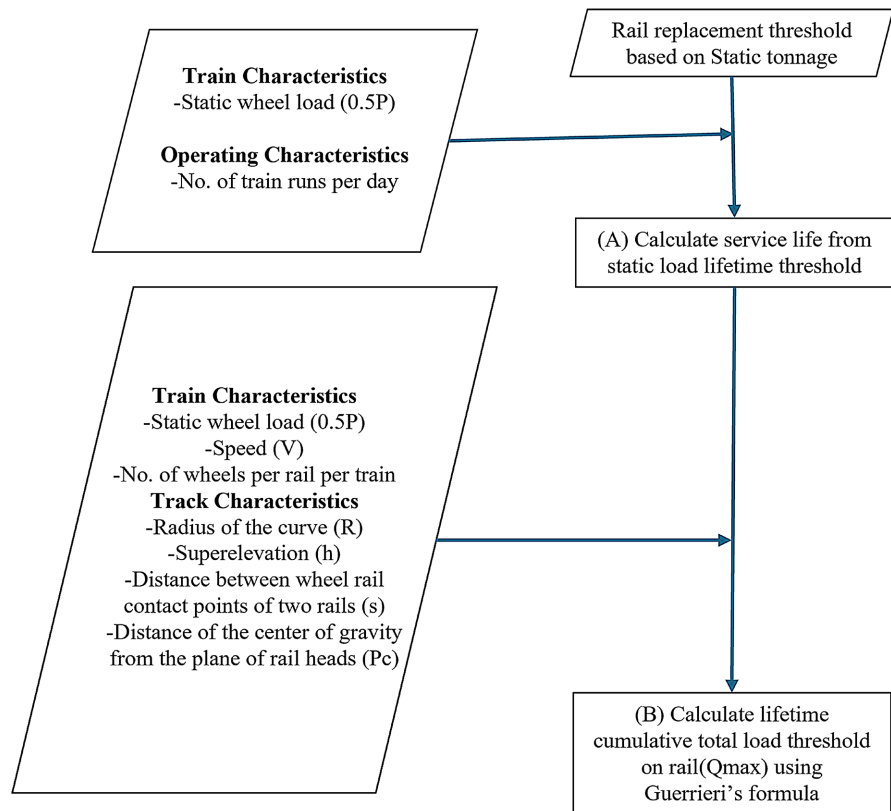


**Figure 2.** Flowchart illustrating the procedure to calculate maximum load criteria for rail replacement.

$n$  = number of wheels per rail.

$N_L$  = rail life in no. of trains.

$$N_Y = N_L / (365 * N_d) \tag{3}$$

where  $N_d$  = number of trains passes per day.

B. Calculation of lifetime cumulative total load threshold on rail,  $Q_{max}$ .

Step 3: Curve-induced load per wheel

$$Q_{av} = P * (P_c * j) / s^2 \tag{4}$$

where  $P$  is the axle load.

$P_c$  is the vertical distance from the rail head plane to the vehicle's center of gravity.

$j$  is the superelevation deficiency, which is calculated using Equation (5) below.

$s$  is the distance between the two rails at the wheel contact points.

Superelevation deficiency ( $j$ ):

$$j = \left\{ (s * v^2) / (g * R) \right\} - h \tag{5}$$

where  $s$  is the distance between the two rails at the wheel contact points.

$v$  is the operating speed of the train.

$g$  is the acceleration due to gravity.

$R$  is the minimum radius of the curve.

$h$  is the superelevation of the curve.

Step 4: Quasi-static load per wheel

$$Q_{qs} = Q_{st} + Q_{av} + Q_v \quad (6)$$

where  $Q_{st}$  is the static load per wheel.

$Q_{av}$  is the vertical load induced when trains run on a horizontal curve.

$Q_v$  is the load induced due to wind, which is not included in this study.

Step 5: Dynamic amplification factor (adopted from Guerrieri [18])

$$DAF = 1 + \left(4.5v^2/100000\right) - \left(1.5v^2/10000000\right) \quad \text{for } v > 100 \text{ km/h} \quad (7)$$

where  $v$  is the operating speed of the train.

Step 6: Dynamic load per wheel

$$Q_{vd} = (DAF - 1) * (Q_{st} + Q_{av}) \quad (8)$$

Step 7: Total vertical load per wheel

$$Q_e = Q_{qs} + Q_{vd} \quad (9)$$

where  $Q_{qs}$  is the quasi-static load (KN).

$Q_{vd}$  is the dynamic load component (KN).

Step 8: Total lateral load per wheel

$$Q_{lat} = DAF * (P * j/s) \quad (10)$$

Note that  $Q_{lat} = Y_e$  in **Figure 1**.

Step 9: Total resultant load per wheel

$$Q_{res} = \sqrt{Q_e^2 + Q_{lat}^2} \quad (11)$$

Step 10: Total load per train

$$Q_{train} = Q_{res} * n \quad (12)$$

where  $Q_{res}$  is the total resultant load per wheel per rail.

$n$  is the number of wheels per rail.

Step 11: Maximum tonnage threshold.

$$Q_{max} = Q_{train} * N_L \quad (13)$$

where  $Q_{train}$  is the total load per train pass.

$N_L$  is the service life of the rail in number of trains.

### Illustrative Calculation Using Shinkansen System

To demonstrate the applicability of the proposed approach, the first step was to identify a typical rail service life in terms of cumulative axle load tonnage for rail replacement. For this study, the Japanese National Railway (Shinkansen) system was used. Their cumulative tonnage for rail replacement was 600 MGT for 60 kg rails (Shimatake [5]). Although this value originates from an old source, it remains one of the few publicly documented rail replacement thresholds for high-speed rail systems. More recent rail replacement criteria are typically treated as proprietary by infrastructure managers and are not available in the open literature. Consequently, the Shimatake threshold is used here as a representative reference value to demonstrate the framework rather than to prescribe an updated policy limit.

Importantly, the proposed methodology is not tied to this specific threshold; it is fully adaptable and can be directly applied with any rail replacement criteria adopted by an infrastructure manager when more recent or system-specific data become available. Additional Shinkansen data that was required for analysis included operating and train characteristics and these were obtained from Suyama [19]; and UIC [20]. The vehicle center of gravity, not directly reported, was assumed to be 1.3 m, consistent with published floor height ranges for modern high-speed trainsets, such as N700, AGV and Velaro [21]. All these data are listed in **Table 1**.

**Table 1.** Summary of Shinkansen parameteres used in maximum load criteria determination.

Parameter	Unit	Value
Rail replacement tonnage threshold, $Q_{threshold}$	MGT	600
Train characteristics		
Axle load per wheelset, $P$	KN	118
	tonnes	12
Number of wheels per train per rail, $n$	-	64
Train operating speed, $v$	km/h	270
Vehicle center of gravity height, $P_c$	m	1.30
Track characteristics		
Track curve radius, $R$	m	2500
Track superelevation, $h$	m	0.20
Wheelset gauge (distance between rails), $s$	m	1.50
Acceleration due to gravity, $g$	m/s <sup>2</sup>	9.81
Operating characteristics		
Train passes per day, $N_d$	-	288

Step 1:

$$Q_{st} = 0.5P = 0.5 * 12 = 6 \text{ tonnes} = 59 \text{ KN}$$

Step 2:

$$N_y = N_L / (365 * N_d) = 1562500 / (365 * 288) = 14.9 \text{ years}$$

Step 3:

$$j = \left\{ \frac{(s * v^2)}{(g * R)} \right\} - h$$

$$= \left[ \left\{ \frac{1.50 * (270/3.6)^2}{(9.81 * 2500)} \right\} - 0.20 \right] = 0.144 \text{ m}$$

$$Q_{av} = P * (P_c * j) / s^2 = 118 * (1.30 * 0.14 / 1.50^2) = 9.820 \text{ KN}$$

Step 4:

$$Q_{qs} = Q_{st} + Q_{av} = 59 + 9.55 = 68.82 \text{ KN}$$

Step 5:

$$DAF = 1 + (4.5v^2/100000) - (1.5v^2/10000000)$$

$$= 1 + (4.5 * 270^2/100000) - (1.5 * 270^2/10000000) = 4.27$$

Step 6:

$$Q_{vd} = (DAF - 1) * (Q_{st} + Q_{av}) = (4.27 - 1) * 68.55 = 225.01 \text{ KN}$$

Step 7:

$$Q_e = Q_{qs} + Q_{vd} = 68.82 + 225.01 = 293.8 \text{ KN}$$

Step 8:

$$Q_{lat} = DAF * (P * j/s) = 4.27 * (118 * 0.144/1.50) = 48 \text{ KN}$$

Step 9:

$$Q_{res} = \sqrt{Q_e^2 + Q_{lat}^2} = \sqrt{293.8^2 + 48^2} = 298 \text{ KN}$$

Step 10:

$$Q_{train} = Q_{res} * n = 298 * 64 = 19058 \text{ KN} = 1944 \text{ tonnes}$$

Step 11:

$$Q_{max} = Q_{train} * N_L = 1944 * 1562500 = 3037102122 \text{ tonnes} = 3037 \text{ MGT}$$

The computed value of  $Q_{max}$  of 3037 MGT represents the cumulative tonnage threshold for rail replacement under the combined influence of axle load, operating speed, and curvature-related dynamic effects. By capturing these load components in a single resultant measure,  $Q_{max}$  provides a more realistic indicator of when rail renewal is required. In the subsequent cost-allocation framework, this threshold is used to determine the rail service life under shared operations and to proportionally assign annualized rail-replacement costs based on each operator's contribution to cumulative loading.

### 3.2. Access Charge Model

The second part of the methodology uses the maximum cumulative tonnage threshold ( $Q_{max}$ ) obtained in Section 3.1 to determine access charges for a shared high-speed rail corridor. The framework computes each operator's contribution to annual rail loading and allocates renewal costs proportionally. **Figure 3** summarizes the procedure.

Following are the steps to calculate the access charge for a shared high-speed rail system:

Step 1: Annual tonnage on the rail based on shared operation

Tonnage per year,

$$Q_{TOT} = \sum_{i=1}^m N_i * Q_i * 365 \tag{14}$$

where  $N_i$  is the average number of trains passing per day for train type  $i$

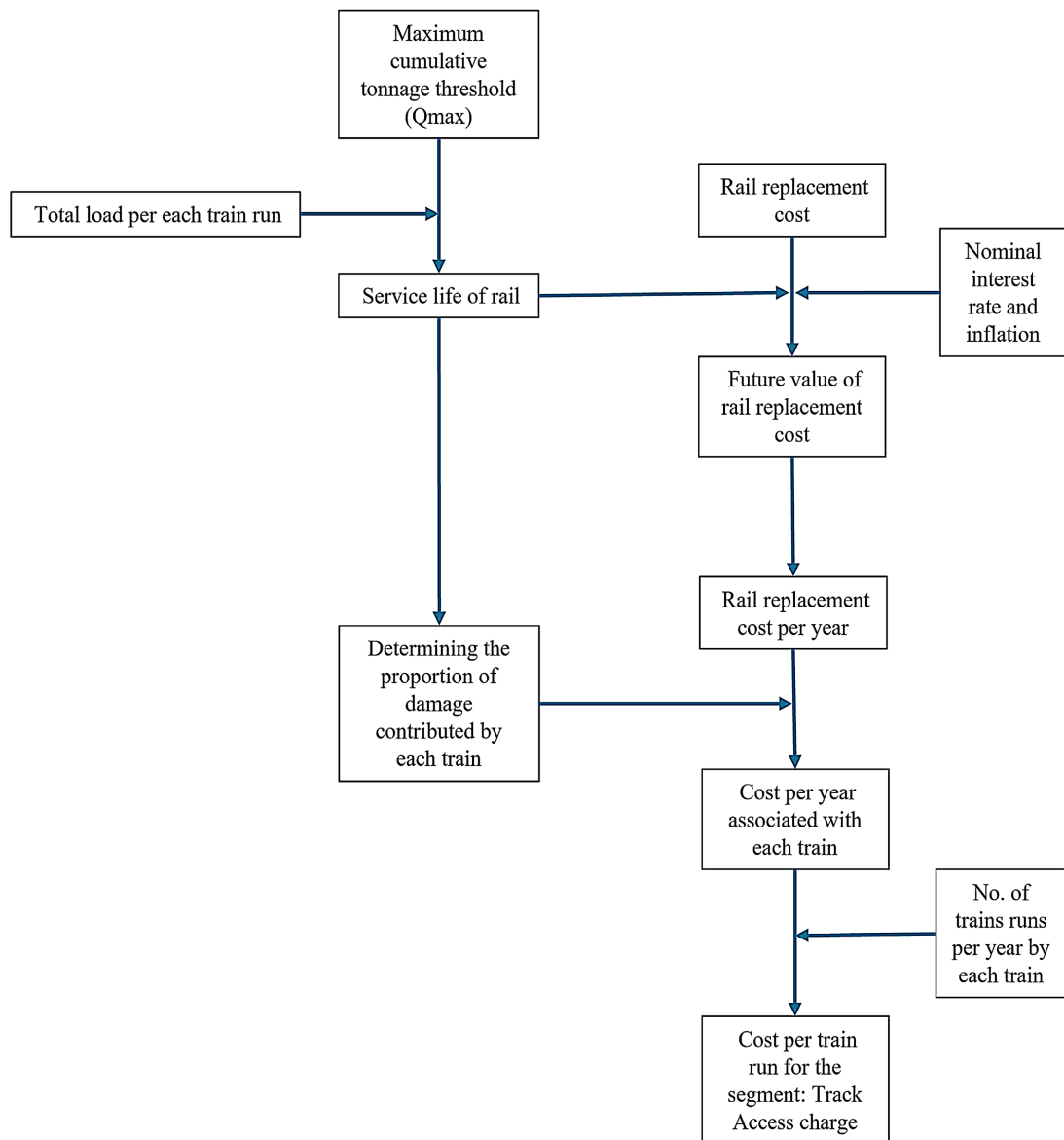


**Figure 3.** Flowchart illustrating the procedure to calculate the access charge.

$Q_i$  is the total load per train pass of train  $i$  (tonnes), calculated as shown in Section 3.1.

$m$  is the number of train types in the shared system.

Step 2: Fraction of the total load for each train type  $i$

$$f_i = (N_i * Q_i * 365) / Q_{TOT} \tag{15}$$

where  $\sum_{i=1}^m f_i = 1$ .

$N_i$  is the number of train passes per day for train type  $i$ .

$Q_i$  is the total load per train pass of train  $i$ .

Step 3: Projected service life of the rail,  $Y_R$  (in years)

$$Y_R = Q_{max} / Q_{TOT} \tag{16}$$

Step 4: Total rail replacement cost at present

$$C_{total} = L * C_{unit} \quad (17)$$

where  $C_{unit}$  is the current unit cost per mile of replacing the rail.

$L$  is the length of the track (miles).

Step 5: Total rail replacement cost in future

Accounting for inflation, the projected cost at the end of service life is:

$$C_{ftotal} = C_{total} * (1 + e)^{Y_R} \quad (18)$$

where  $e$  is the average annual inflation rate over the  $Y_R$  years.

Step 6: Equivalent uniform annual cost of rail replacement

$$C_{FV} = C_{ftotal} * d / \{(1 + d)^{Y_R} - 1\} \quad (19)$$

where  $d$  is the effective nominal discount rate.

Step 7: Annual access charges for train,  $i$  based on their contribution of load

$$C_{FVi} = f_i * C_{FV} \quad (20)$$

Step 8: Access charge per train pass of train type  $i$

$$C_{trip,i} = C_{FVi} / (N_i * 365) \quad (21)$$

Step 9: Access charge per train mile for train type  $i$

$$C_{train-mile,i} = C_{trip,i} / L \quad (22)$$

where  $L$  is the length of the shared track segment.

This stepwise formulation ensures transparency and fairness by charging operators in proportion to their actual contribution to rail deterioration, rather than relying on simple distance or gross-tonnage proxies.

## 4. Case Study of Palmdale to Burbank Proposed Shared Track Segment

### 4.1. Overview of the Case Study Corridor

To demonstrate the practical application of the proposed framework, we applied the methodology to the planned Palmdale-Burbank segment of the California High-Speed Rail (CAHSR) project. This 41-mile corridor, part of CAHSR Phase 1, connects California's Central Valley with the Los Angeles Basin through mountainous terrain that requires multiple tunnels. Its strategic location makes it an essential link for integrating north-south passenger travel across the state.

This section was selected because of its potential for shared operation between the public CAHSR system and a private operator (Brightline West, which, at the time this research was being conducted, was developing an electrified high-speed line between Las Vegas and Southern California). Although concrete plans for joint operation remain conceptual, this scenario provides an ideal context to evaluate how the load-based access charge framework can allocate rail replacement costs between multiple high-speed services that differ in axle load, operating speed, and frequency.

## 4.2. Case Study Data and Assumptions

As the CAHSR Authority currently defines a time-based rail replacement cycle of approximately 50 years without an explicit tonnage limit, this study applies the Shinkansen reference threshold of 600 MGT [5], adjusted using the derived load model to a maximum cumulative tonnage ( $Q_{\max}$ ) of 3,037 MGT.

Train, track, and operating parameters were compiled from CAHSR and Brightline West project documents [22] [23], supplemented by standard high-speed rail design guidelines when specific data were not available. In this model, CAHSR trains have a 17-ton axle load and run 40 trains per day, representing a high-capacity intercity service. Brightline West trains were assumed to have a 15-ton axle load and 20 trains per day, reflecting a lighter, medium-frequency operation. All the data required for the calculation are listed in **Table 2** below.

**Table 2.** Summary of case study parameters used in maximum load criteria determination.

Parameter	Unit	CAHSR	Brightline West
Rail replacement tonnage threshold, $Q_{\max}$	MGT	3037	
Train characteristics			
Axle load per wheelset, $P$	KN	169	149
	tonnes	17	15
Number of wheels per train per rail, $n$	-	64	32
Train operating speed, $v$	km/h	350	320
Vehicle center of gravity height, $P_c$	m	1.40	1.4
Track characteristics			
Track curve radius, $R$	m	3000	3000
Track superelevation, $h$	m	0.20	0.20
Wheelset gauge (distance between rails), $s$	m	1.50	1.50
Acceleration due to gravity, $g$	m/s <sup>2</sup>	9.81	9.81
Operating characteristics			
Train passes per day, $N$	-	40	20

## 4.3. Calculation of Train Loads for Shared Use

Using the methodology from Section 3, total wheel-rail loads were computed for both train types under curved track conditions representative of the Palmdale-Burbank segment which is shown in **Table 3** along with the calculation. This analysis captures the combined effects of track curvature, superelevation, and dynamic amplification, which together determine the resultant wheel loads that govern rail wear and replacement.

The results show that each CAHSR train imposes approximately three times the total resultant load per pass compared to each Brightline West train. With CAHSR also running twice as many trains per day, it accounts for roughly 85% of the total

cumulative loading on the shared track. Including lateral forces increases the resultant load magnitude by about 4% - 6% compared to a vertical-only model, highlighting the importance of accounting for track curvature effects when estimating  $Q_{max}$  and rail service life.

**Table 3.** Load calculation of the CAHSR and Brightline West.

Parameter	Equation	CAHSR	Brightline West	Unit	
Train characteristics					
Axle load per wheelset	$P$	169	149	KN	
		17	15	tonnes	
Number of wheels per train per rail	$n$	64	32	-	
Train operating speed	$v$	350	320	km/h	
Vehicle center of gravity height	$P_c$	1.4	1.4	m	
Track characteristics					
Track curve radius	$R$	3,000	3,000	m	
Track superelevation	$h$	0.2	0.2	m	
Wheelset gauge	$s$	1.5	1.5	m	
Acceleration due to gravity	$g$	9.81	9.81	m/s <sup>2</sup>	
Operating characteristics					
Train passes per day	$N_d$	40	20	-	
Calculations					
Static wheel load	$Q_{st}$	$0.5 * P$	84.5	74.5	KN/wheel
			8.5	7.5	tonnes/wheel
Superelevation deficiency	$j$	$\frac{s * v^2}{g * R} - h$	0.282	0.203	m
Additional load on horizontal curve	$Q_{av}$	$P * \frac{P_c * j}{s^2}$	29.629	18.794	KN/wheel
Quasi static load	$Q_{qs}$	$Q_{st} + Q_{av}$	114.13	93.29	KN/wheel
Dynamic amplification factor	$DAF$	$1 + \frac{4.5v^2}{100000} - \frac{1.5v^2}{10000000}$	6.494	5.593	-
Vertical dynamic wheel load	$Q_{vd}$	$(DAF - 1) * (Q_{st} + Q_{av})$	627.04	428.46	KN/wheel
Total vertical load per wheel	$Q_e$	$Q_{qs} + Q_{vd}$	741.2	521.8	KN/wheel
Total lateral load per wheel	$Q_{lat}$	$DAF * \left( P * \frac{j}{s} \right)$	206	113	KN/wheel
Total resultant load per wheel	$Q_{res}$	$\sqrt{Q_e^2 + Q_{lat}^2}$	769	534	KN/wheel
Total load per train	$Q_{train}$	$Q_{res} * n$	49,235	17,081	KN/train
			5021	1742	tonnes/train

#### 4.4. Calculation of Access Charge

The total rail replacement cost for the Palmdale-Burbank section was derived from the California High Speed Rail Authority (CHSRA) Capital Cost Basis of Estimate [24] and 50-Year Lifecycle Capital Cost reports [25]. Because the segment likely includes a mix of ballasted and slab track, a 50:50 split was assumed. Using renewal cost factors of 36% of the initial cost for ballasted track and 25% for slab track, the base rail replacement cost ( $C_{total}$ ) was estimated at USD 37.75 million. Economic parameters adopted for this analysis include an annual inflation rate ( $e$ ) of 3 % and nominal discount rate ( $d$ ) of 4 %. **Table 4** summarizes the key cost inputs and economic assumptions used in the access charge calculation and **Table 5** summarizes the results of the case study.

**Table 4.** Input parameters for the calculation of the access charge.

Parameter	Value
Segment length	41 miles
Rail replacement cost for the shared segment ( $C_{total}$ )	\$37,752,582
Nominal interest rate	4 %
Inflation rate	3 %

**Table 5.** Summary of cost calculation for CAHSR and brightline west.

Parameter	CAHSR	Brightline West
Damage fraction	0.85	0.15
Annual cost	\$1,119,019	\$211,030
Daily train passes	40	20
Yearly train passes	14,600	7300
Access charge per train trip	\$82.12	\$28.91
Access charge per train trip	\$2.00	\$0.71

Step 1: Annual tonnage on the rail based on shared operation

Tonnage per year,

$$Q_{TOT} = \sum_{i=1}^m N_i * Q_i * 365 = 40 * 5021 * 365 + 20 * 1742 * 365 = 86023200 \text{ tonnes}$$

Step 2: Fraction of the total load for each train type

$$f_{CAHSR} = (N_i * Q_i * 365) / Q_{TOT} = (40 * 5021) / (40 * 5021 + 20 * 1742) = 0.85$$

$$f_{BrightlineWest} = (N_i * Q_i * 365) / Q_{TOT} = (20 * 1742) / (40 * 5021 + 20 * 1742) = 0.15$$

Step 3: Projected service life of the rail, YR

$$Y_R = Q_{max} / Q_{TOT} = 3037 \text{ MGT} / 86023200 \\ = 3037 * 10^6 / 86023200 = 35.30 \approx 36 \text{ years}$$

Step 4 was omitted in this case because the total rail replacement cost for the

entire shared segment was directly available, eliminating the need to use a unit cost per mile.

Step 5: Total rail replacement cost in the future

$$C_{total} = C_{total} * (1 + e)^{Y_R} = \$37752582 * (1 + 0.03)^{36} = \$109417489$$

Step 6: Equivalent uniform annual cost of rail replacement

$$C_{FV} = C_{total} * d / \{(1 + d)^{Y_R} - 1\} = \$109417489 * 0.04 / \{(1 + 0.04)^{36} - 1\} = \$1410050$$

Step 7: Annual access charges for each train based on their contribution of load,

$$C_{FV,CAHSR} = f_{CAHSR} * C_{FV} = 0.85 * \$1410050 = \$1119019$$

$$C_{FV,BrightlineWest} = f_{BrightlineWest} * C_{FV} = 0.15 * \$1410050 = \$211030$$

Step 8: Access charge per trip of train type *i*,

$$C_{trip,CAHSR} = C_{FV,CAHSR} / (N_{CAHSR} * 365) = \$1119019 / (40 * 365) = \$82.12$$

$$C_{trip,BrightlineWest} = C_{FV,BrightlineWest} / (N_{BrightlineWest} * 365) = \$211030 / (20 * 365) = \$28.91$$

Step 9: Access charge per train mile for train type *i*,

$$C_{train-mile,CAHSR} = C_{trip,CAHSR} / L = \$82.12 / 41 = \$2.00$$

$$C_{train-mile,BrightlineWest} = C_{trip,BrightlineWest} / L = \$28.91 / 41 = \$0.71$$

These results show how the framework converts calculated rail wear into a fair and transparent access charge for each operator.

#### 4.5. Effects of Neglecting Dynamic Loads on Rail Service Life

To illustrate the influence of dynamic and lateral loading, a comparative calculation was performed using only static wheel loads. The results are summarized in **Table 6**, which shows the cumulative tonnage and corresponding rail service life when dynamic and lateral effects are omitted. Under these conditions, the estimated rail service life is overestimated to approximately 62 years. For comparison, the full framework, which incorporates dynamic vertical load effects associated with operating speed, curvature-related loading, and lateral forces, yields a service life of approximately 36 years for the case study conditions.

The difference between these two values shows that excluding dynamic and lateral components produces a significantly overestimated longer service-life estimate.

#### 4.6. Summary of Case Study Findings

The case study illustrates how the proposed load-based access charge framework translates physical rail deterioration into a transparent and equitable cost allocation model. The higher charge assigned to CAHSR stems directly from its higher dynamic and lateral loads and greater number of train passes, aligning with the cost-causation principle. When the effects of dynamic and lateral forces are ignored, the estimated rail service life is unrealistically high at about 62 years, an overestimation of nearly 70% relative to the 36 years estimate based on analysis

**Table 6.** Rail service life neglecting the dynamic loads.

Parameter	Equation	CAHSR	Brightline West	Unit
Inputs				
Rail life threshold	$Q_{\text{threshold}}$		600	MGT
Axle load per wheelset	$P$	17	15	tonnes
Number of wheels per train per rail	$n$	64	32	-
Train passes per day	$N_d$	40	20	-
Calculations				
Static wheel load	$Q_{st} = 0.5 * P$	8.5	7.5	tonnes/wheel
Total load per train	$Q_{st} * n$	544	240	tonnes/train
Total load per day	$Q_{st} * n * N_d$	21,760	4800	tonnes
Total load combined	$\sum Q_{st} * n * N_d$		26,560	tonnes
Rail service life	$\frac{\sum Q_{st} * n * N_d}{Q_{\text{threshold}}}$		61.9 years	years

with dynamic loads. This highlights the critical role of dynamic load components in accurately representing rail deterioration under real operating conditions.

Although the calculated access charges cover only rail replacement costs, excluding ballast, sleeper, and signaling maintenance, they remain at the lower bound of international high-speed rail access fees. For comparison, full O&M-inclusive rates in France, Germany, and Italy are approximately USD 42.8, 24.9, and 10.8 per train-mile, respectively [11]. These results demonstrate the framework's internal consistency and its practical scalability to U.S. contexts.

Beyond financial equity, the findings have operational implications. By incorporating dynamic and lateral load effects, the framework links physical degradation directly to traffic characteristics, enabling infrastructure managers to plan renewal cycles and pricing structures more effectively. The Palmdale-Burbank case highlights how shared high-speed corridors could balance private and public participation under performance-based (rather than policy-based) cost frameworks.

## 5. Discussion

The findings of this study demonstrate the critical importance of incorporating dynamic and curvature-induced effects when determining rail deterioration and cost allocation on shared high-speed corridors. Traditional approaches to access charging often rely on gross tonnage or distance-based proxies, overlooking how train speed, axle load, and track geometry can magnify rail stress. The proposed framework integrates these factors through dynamic amplification and resultant wheel-rail loading, allowing the cumulative tonnage threshold ( $Q_{\text{max}}$ ) to reflect actual operating conditions. This improvement enables infrastructure managers to

plan renewals based on actual mechanical wear rather than fixed time intervals, establishing a more accurate link between service parameters and asset life. Neglecting the effects of speed and curvature-induced dynamics was found to substantially overestimate rail service life: when only static loads were considered, the predicted lifespan increased from 36 years to 61.9 years—an overestimation of nearly 70%. This finding underscores the importance of explicitly incorporating dynamic and lateral forces to obtain realistic rail life estimates and accurate maintenance planning.

From an implementation perspective, the framework relies on operational data that are routinely available to infrastructure managers or can be specified contractually for shared-use corridors. Key inputs include axle load and train configuration (number of wheels), operating speed, service frequency, and basic track geometry such as curve radius, superelevation and track gauge. These parameters are typically defined during rolling stock certification, timetable planning, and infrastructure design, and are already used for safety, capacity, and maintenance management purposes. As a result, applying the proposed framework does not require new measurement systems, but rather integrates existing engineering and operational data into a unified cost-allocation process.

In addition to the engineering implications, the framework provides an economic mechanism that translates physical wear into equitable financial responsibility. By converting future renewal costs into an equivalent uniform annual cost and apportioning them based on each operator's share of the cumulative load, the model ensures transparent, performance-based pricing. Services that exert greater dynamic stress on the rail bear proportionally higher access charges, while lighter or slower services pay less. This approach upholds the cost causation principle and supports financially sustainable infrastructure management by aligning technical deterioration with long-term cost recovery. It also offers policymakers a defensible basis for negotiating fair access agreements between public and private operators on shared high-speed networks.

While the framework focuses on rail replacement costs driven by physical loading, the resulting access charges are also influenced by economic assumptions used in the life-cycle cost calculation, particularly the inflation and discount rates. These parameters affect the annualized replacement cost but do not alter the relative cost allocation among operators, which is governed by their respective contributions to cumulative rail loading. As a result, variations in economic inputs primarily scale the magnitude of access charges rather than changing the proportional responsibility assigned to each service. This distinction allows infrastructure managers to update financial assumptions over time without modifying the underlying load-based allocation logic.

The application of this framework to the Palmdale-Burbank segment of California's proposed high-speed system illustrates its real-world relevance. Results indicate that the California High-Speed Rail (CAHSR) service, operating with higher axle loads and speeds, accounts for approximately 85% of total rail wear,

whereas Brightline West contributes about 15%. The corresponding access charges are estimated at USD 2.00 per train-mile for CAHSR and USD 0.71 per train-mile for Brightline West align with their proportional load contributions and fall within the lower range of international access fee benchmarks. Although the current model considers only rail replacement costs, it can be scaled to integrate additional infrastructure components such as ballast, sleepers, and overhead systems in future work. Overall, the study demonstrates that incorporating realistic train dynamics into access charge frameworks promotes fairness, transparency, and long-term sustainability in shared high-speed rail operations.

## 6. Conclusion and Future Recommendations

This study developed a load-based framework for determining equitable track access charges on shared high-speed rail corridors. The model integrates both static and dynamic wheel-rail interactions, capturing the combined effects of axle load, train speed, and track geometry on the static and dynamic loads on the rails. Unlike conventional access charge approaches that rely solely on gross tonnage or distance, this framework links the loading that rails are subjected to directly to train-specific operating parameters, providing a more realistic measure of infrastructure usage.

The use of this framework was illustrated through a case study on the Palmdale-Burbank corridor of the planned and under construction California High Speed Railway network. It resulted in proportional allocation of estimated rail replacement costs as a function of the characteristics of each train system, in terms of the operating speeds, axle loads and frequency of service. The approach effectively translated engineering parameters into proportional financial contributions, enabling transparent, performance-based cost allocation among multiple operators thus improving economic fairness in shared high-speed rail systems.

One of the key limitations of this framework is that it implies that rail wear and tear is proportional to the static and dynamic vertical and lateral loading that the rail is subjected to, which may or may not be the case. Since rail replacement and maintenance costs are a function of rail and track damage, not just rail loading, there is therefore a need for further research to relate rail wear and tear to the rail loading and update this framework accordingly. Also, future research should extend this model beyond rail replacement to include other key infrastructure components, such as ballast, sleepers, and fasteners, thereby providing a more comprehensive life-cycle cost framework.

## Acknowledgements

This paper is derived from the author's Master's thesis completed in the Department of Civil and Environmental Engineering at the University of Nevada, Las Vegas [7]. The authors acknowledge the support and academic environment that facilitated this research.

## Conflicts of Interest

The authors declare no conflicts of interest regarding the publication of this paper.

## References

- [1] International Union of Railways (UIC) (2023) High-Speed Around the World Historical, Geographical, and Technological Development.
- [2] Akiyama, Y. (2014) 50 Years of High-Speed Railways High-Speed Rail Worldwide—Past and Future High-Speed Rail: A Start in Japan Global Spread. *Japan Railway & Transport Review*, No. 64, 36-47.
- [3] Smith, A., Iwnicki, S., Kaushal, A., Odolinski, K. and Wheat, P. (2017) Estimating the Relative Cost of Track Damage Mechanisms: Combining Economic and Engineering Approaches. *Proceedings of the Institution of Mechanical Engineers, Part F: Journal of Rail and Rapid Transit*, **231**, 620-636. <https://doi.org/10.1177/0954409717698850>
- [4] Ralbovsky, M. and Morga, M. (2012) Dynamic Train Wheel Forces: Numerical Parameter Study. *Proceedings of the ISMA 2012 International Conference on Noise and Vibration Engineering*, Leuven, 17-19 September 2012.
- [5] Shimatake, M. (1997) A Track Maintenance Model for High-Speed Rail: A System Dynamics Approach. Master's Thesis, Massachusetts Institute of Technology.
- [6] Van Dyk, B.J., Edwards, J.R., Dersch, M.S., Ruppert, C.J. and Barkan, C.P. (2016) Evaluation of Dynamic and Impact Wheel Load Factors and Their Application in Design Processes. *Proceedings of the Institution of Mechanical Engineers, Part F: Journal of Rail and Rapid Transit*, **231**, 33-43. <https://doi.org/10.1177/0954409715619454>
- [7] Yadav, N.K. (2025) Development of an Access Charge Framework for High-Speed Rail Incorporating Rail Replacement Costs and Dynamic Train Characteristics. Ph.D. Thesis, University of Nevada, 8-15.
- [8] Ehrhart, U., Knabl, D. and Marschnig, S. (2024) Track Deterioration Model—State of the Art and Research Potentials. *Infrastructures*, **9**, Article 86. <https://doi.org/10.3390/infrastructures9050086>
- [9] López-Pita, A. and Robusté, F. (2003) Effect of Very High-Speed Traffic on the Deterioration of Track Geometry. *Transportation Research Record: Journal of the Transportation Research Board*, **1825**, 22-27. <https://doi.org/10.3141/1825-04>
- [10] Lyon, D. (2002) Engineering Review of Vertical Dynamic Track Forces. ITLR Report No. ITLR/T11289/001, Order No. IFLT/111257.
- [11] Boyapati, K.S.T. (2020) Analysis of High-Speed Rail Operations Using Vissim Simulation to Determine Access Charges and the Impact of Incidents on a Shared Network. Ph.D. Thesis, University of Nevada.
- [12] Federal Office of Transport (BAV) (2022) Base Price Wear in the Train-Path Pricing System Instructions for Determining Vehicle Prices. Version 1.1.
- [13] Marschnig, S. (2016) Innovative Track Access Charges. *Transportation Research Procedia*, **14**, 1884-1893. <https://doi.org/10.1016/j.trpro.2016.05.155>
- [14] Sapkota, S. (2018) Calculation of Access Charge for High-Speed Rail Xpresswest of Nevada. Ph.D. Thesis, University of Nevada.
- [15] Marschnig, S., Vidovic, I. and Vidović, I. (2019) Estimating Future Tamping Demands Using the Swiss Wear Factor. <https://www.researchgate.net/publication/339800465>

- 
- [16] Johansson, P. and Nilsson, J. (2004) An Economic Analysis of Track Maintenance Costs. *Transport Policy*, **11**, 277-286. <https://doi.org/10.1016/j.tranpol.2003.12.002>
- [17] Northeast Corridor Commission (NEC) (2024) Northeast Corridor Commuter and Intercity Rail Cost Allocation Policy. [https://nec-commission.com/wp-content/uploads/2025-07-08\\_Cost-Allocation-Policy\\_v14.00\\_For-Publication-1.pdf](https://nec-commission.com/wp-content/uploads/2025-07-08_Cost-Allocation-Policy_v14.00_For-Publication-1.pdf)
- [18] Guerrieri, M. (2023) Fundamentals of Railway Design. in Springer Tracts in Civil Engineering. Springer.
- [19] Suyama, Y. (2014) 50 Years of High-Speed Railways. *Japan Railway & Transport Review*, No. 64, 18-29.
- [20] UIC (2018) World High Speed Rolling Stock. [https://uic.org/IMG/pdf/20180910\\_highspeed\\_rolling\\_stock.pdf](https://uic.org/IMG/pdf/20180910_highspeed_rolling_stock.pdf)
- [21] California High Speed Rail Authority (2023) California High-Speed Train Project Technical Memorandum Trainset Configuration Analysis and Recommendation TM 6.3. [https://hsr.ca.gov/wp-content/uploads/docs/programs/eir\\_memos/Proj\\_Guidelines\\_TM6\\_3R00.pdf](https://hsr.ca.gov/wp-content/uploads/docs/programs/eir_memos/Proj_Guidelines_TM6_3R00.pdf)
- [22] California High-Speed Rail Authority (2024) California High-Speed Rail Authority Palmdale to Burbank Project Section Final Environmental Impact Report/Environmental Impact Statement Appendix 2-D Design Baseline Report. [https://hsr.ca.gov/wp-content/uploads/2024/05/PB\\_02.0\\_AppxD\\_PEPD\\_REC-ORD\\_SET\\_Design\\_Baseline\\_Report\\_a11y.pdf](https://hsr.ca.gov/wp-content/uploads/2024/05/PB_02.0_AppxD_PEPD_REC-ORD_SET_Design_Baseline_Report_a11y.pdf)
- [23] Nevada, D.O.T. (2025) Brightline West High Speed Rail Project. <https://www.dot.nv.gov/projects-programs/transportation-projects/brightline-west-high-speed-rail-project>
- [24] California High Speed Rail Authority (2024) 2024 Business Plan-Basis of Estimate. [https://hsr.ca.gov/wp-content/uploads/2024/05/2024\\_Business\\_Plan\\_Basis\\_of\\_Estimate-FINAL.pdf](https://hsr.ca.gov/wp-content/uploads/2024/05/2024_Business_Plan_Basis_of_Estimate-FINAL.pdf)
- [25] California High Speed Rail Authority (2024) 2024 Business Plan 50 Year Lifecycle Capital Cost Model. [https://hsr.ca.gov/wp-content/uploads/2024/02/240208-ETO-LCC-DRAFT-2024-BP-50-Year-Lifecycle-Capital-Cost-Model-CHSRA\\_v01-A11Y.pdf](https://hsr.ca.gov/wp-content/uploads/2024/02/240208-ETO-LCC-DRAFT-2024-BP-50-Year-Lifecycle-Capital-Cost-Model-CHSRA_v01-A11Y.pdf)

## Appendix 1: Representative Axle Loads and Speeds of High-Speed Trains

The data in **Table A1** is extracted from the World High-Speed Rolling Stock database published by the International Union of Railways [20]. It presents representative axle loads and maximum speeds for various high-speed trains operating globally.

**Table A1.** Representative axle loads and speeds of high-speed trains.

Country	Owners or Operators	Class	Train set Formula	Max. Train Speed (Km/h)	Max. Axle Load (tonnes)
France	SNCF	TGV Atlantique	2L10T	300	17
Germany	DB AG	401(ICE1)	2L12T	280	19.5
Italy	Trenitalia	ETR450	8M1T	250	12.5
Spain	Renfe Operadora	S100(bic)	2L8T	300	17.2
China	CR	CRH1B	10M6T	250	16.5
Japan	JRW	0	6M	220	16
Japan	JRW	100	6M	230	15
Japan	JRE	200	10M	240	16.4
Japan	JRC, JRW	300, 300-3000	10M6T	270	12
Japan	JRE	400	6M1T	240	12.9
Japan	JRW	500	16M	300	11.7
Japan	JRC, JRW	700, 700-3000	12M4T	285	11.4
Japan	JRW	700-7000	6M2T	285	11.4
Japan	JRC, JRW	N700, -2000, N700-3000, -5000, N700A (N700-1000, N700-4000)	14M2T	300	11.4

## Appendix 2: Data Sources for Rail Replacement and Cost Estimation

### A2.1. Capital Cost Estimate for Track Construction

The data in **Table A2** is extracted from Appendix Q of the 2024 Business Plan Basis of Estimate published by the California High-Speed Rail Authority [24]. It provides capital cost estimates for different track construction types:

**Table A2.** Track construction cost for Palmdale to Burbank track segment.

SCC No.	Description	Cost (Dollars)
10.09	Track new construction: Conventional Ballasted	\$97,112,102
10.10	Track new construction: Non-Ballasted	\$162,179,227

### A2.2. Rail Replacement Cost as a Percentage of Capital Cost

The data in **Table A3** is extracted from **Table 3** of the 2024 50-Year Lifecycle Capital Cost Model published by the California High-Speed Rail Authority [25]. It summarizes the percentage of capital cost allocated to track replacement activities over a 50-year period:

**Table A3.** Rail replacement cost as a proportion for Palmdale to Burbank track segment.

No.	Asset Type	2024 Replacement Assumptions	2024 Replace. Years
<b>10.09</b>	Track new construction: Conventional Ballasted		
<b>10.09D</b>	Rail	50 years, 36% of initial capital cost of all 10.09 components, spread over 20 years	50
<b>10.10</b>	Track new construction: Non-ballasted		
<b>10.10C</b>	Rail	50 years, 25% of initial capital cost of all 10.09 components, spread over 20 years	50